Synthesis and Characterization of Poly{1,2-bis(2-seleninyl)ethene}, a Novel Electrically Conductive Polymer with Diminished Band Gap

S. C. Ng,*[†] H. S. O. Chan,[†] T. T. Ong,[†] K. Kumura,[‡] Y. Mazaki,[‡] and K. Kobayashi[‡]

Department of Chemistry, National University of Singapore, Kent Ridge, Singapore 119260, and Department of Chemistry, The University of Tokyo, Komaba, Meguro-ku, Tokyo 153, Japan

Received July 7, 1997

ABSTRACT: A novel electrically conducting polymer containing selenophene and ethenyl spacer, poly-{1,2-bis(2-seleninyl)ethene} (PDSE), has been generated by chemical and electrochemical polymerization. This polymer exhibits a significantly lower band gap (1.61 eV) than polyselenophene and possesses partial solubility in common organic solvents. The electrochemical and optical properties have been thoroughly investigated by cyclic voltammetry and UV−vis spectroscopy. This polymer can be reversibly reduced and oxidized (both n- and p-doped) between −2.0 V and +0.8 V (vs SCE). Chemically doped polymers using chemical reagents such as iodine and ferric chloride afforded materials with a maximum conductivity of 0.27 S cm^{-1}. Scanning electron micrographs of (ClO$_4^-$) doped polymers deposited on indium tin oxide coated glass electrode depict a globular morphology. X-ray photoelectron spectroscopic studies of PDSE were conducted using undoped polyselenophene synthesized from a nickel-catalyzed Grignard cross-coupling reaction as a calibration standard for the Se 3d environment.

Introduction

Research in organic conducting polymers has to date largely focused on polyfuran,[1] polythiophene,[2] polypyrrole,[3] and their functional derivatives, while relatively little work was conducted on higher selenium-containing analogues.[4] Although electron conduction occurs through the extended π-bonded system of the carbon backbone, the nature of the heteroatoms such as S, O, and Se can nevertheless exert a profound influence on the electronic, redox, optical, and mechanical properties and the stability of these polymeric materials. On comparison, the differences in the chemistry of selenium versus sulfur include the increased metallic character, involvement of filled 3d orbitals, and a decrease in the electronegativity of the element. Accordingly, we have initiated a program of structure−property correlation studies on functionalized polyselenophenes, particularly polymers incorporating conjugative spacers such as the ethenyl and ethynyl moieties on the polymer backbone, as an extension of our earlier investigations on related materials.[5] Although there are some literature reports on the pendant functionalized poly(3-alkylselenophenes) (I)[6] (Figure 1) and poly(3-alkoxyselenophenes) (II),[7] we are cognitive of only one brief report on the backbone-modified poly(2,5-selenophenediylvinylene) (III),[8] which is in contrast to the extensive and detailed studies conducted on analogous materials incorporating thiophene[9] and furan[10] moieties. It is anticipated that for such materials, the consequent enhanced conjugation arising from a higher degree of coplanarity due to diminished steric interaction of the ring hydrogens in the β-positions would afford polymers that possess lower band gap energies. Further, since the selenophene moiety has a lower oxidation potential than thiophene, selenophene-containing polymers are likely to undergo more facile doping than analogous thiophene-containing materials. Thus, polymer **III** was reported by Iwatsuki
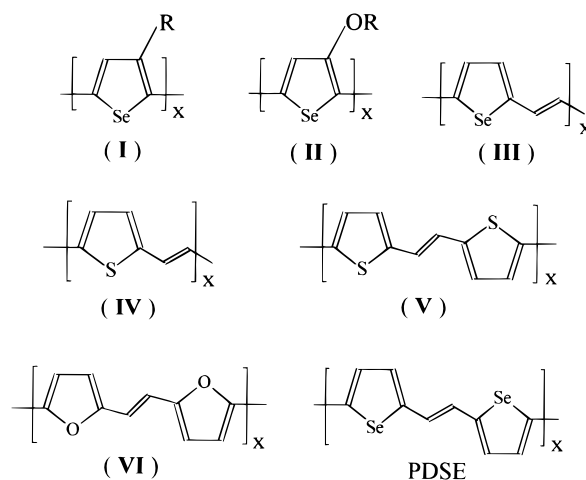

Figure 1. Chemical structures of poly(3-alkylselenophene) (**I**), poly(3-alkoxyselenophene) (**II**), poly(2,5-selenophenediylvinylene) (**III**), poly(2,5-thienylenevinylene) (**IV**), poly{1,2-bis-(2-seleninyl)ethene} (PDSE), poly-{1,2-(2,2′-dithienyl)ethene} (**V**), and poly{1,2-bis(2-furyl)ethene} (**VI**).

et al. to give a conductivity of 330 S cm^{-1} when doped with iodine. This value is much higher than those of the analogous thiophene, polymer **IV**[11] (220 S cm^{-1}). In this regard, we have successfully synthesized the novel poly{1,2-bis(2-seleninyl)ethene} (PDSE) for comparison with poly{1,2-bis(2,2′-dithienyl)ethylene} (**V**)[12] and poly-{1,2-bis(2-furyl)ethene} (**VI**).[13] Polymer **V** has been reported by Onoda et al. to have a band gap of 1.9 eV.[14] The conductivity of its unsubstituted and alkyl-substituted polymer is 0.1 S cm^{-1} when doped with iodine. The furan analogue (**VI**) of PDSE was reported by Kossmehl and Greczmiel to be semiconducting (2 × 10^{-5} S cm^{-1}) when doped with ferric chloride. PDSE, on the other hand, achieved a maximum conductivity of 0.27 S cm^{-1} when iodine doped and has an optical band gap of 1.6 eV.

We report here our findings on PDSE, which has been generated through both chemical and electrochemical methods. The XPS studies of PDSE are also detailed,

* Author for correspondence.
[†] National University of Singapore.
[‡] The University of Tokyo.

which to our knowledge were not presented elsewhere for selenophene-containing polymers. It has been determined also that PDSE demonstrates good potential suitable use as materials in rechargeable batteries,[15] electrochromic devices,[16] and supercapacitors.[17] For most polymers, the p-doping activity has been well researched while the n-type doping studies are comparatively rare due to the poor stability of the polymer at extreme negative potentials. Nevertheless, PDSE is able to exhibit facile p- and n-doping capabilities at the potential range between −2.0 and +0.8 V. This property makes it a suitable material for exploratory work in the construction of type III capacitors,[18] whereby one electrode is p-doped and the other is n-doped when the capacitor is charged.

Experimental Section

Materials. Anhydrous ferric chloride (Merck) and *N*-bromosuccinimide (Merck) were used as received. Electrochemical electrolytes, Bu₄NBF₄ (TCI), Bu₄NClO₄ (TCI), Bu₄NSO₃CF₃ (TCI), and LiClO₄ (Merck), were dried under high vacuum at 60 °C for 24 h prior to use. Chloroform (J. T. Baker), acetonitrile (J. T. Baker), and nitromethane (Merck) were reagent grade solvents and freshly distilled over calcium hydride. Tetrahydrofuran (J. T. Baker), dimethylformamide (J. T. Baker), dimethyl sulfoxide (J. T. Baker), and *N*-methylpyrrolidone (TCI) are reagent grade solvents unless otherwise stated. Polyselenophene in its fully undoped state was obtained as previously reported by Bezoari et al.[19] using a nickel-catalyzed Grignard cross-coupling reaction.

Elemental Analysis. All monomer and polymer samples were analyzed at the NUS Microanalytical Laboratory on a Perkin-Elmer 240C elemental analyzer for C, H, S, and N determinations. Halogen determination was done either by ion chromatography or the oxygen flask method.

Infrared Spectroscopy. FT-IR spectra of monomers and polymers were dispersed in KBr disks and recorded on a Perkin-Elmer 1600 spectrometer.

Ultraviolet−Visible Absorption Spectroscopy. UV−vis spectra were obtained from dilute solutions or thin films deposited electrochemically on an indium tin oxide (ITO) coated glass plate on a Shimadzu UV-160 spectrophotometer.

Thermogravimetry. Thermogravimetric analyses (TGAs) of polymer powders were conducted on a DuPont Thermal Analyst 2100 system with a TGA 2950 thermogravimetric analyzer. A heating rate of 10 °C with an air flow of 75 mL min⁻¹ was used. The runs were conducted from room temperature to 800 °C.

Electrical Conductivity Measurements. Conductivity measurements were carried out on polymer pellets of a known thickness (ca. 0.5 mm) using a four-point probe connected to a Keithley constant current source system. Conductivities were calculated on the basis of the average of at least 10 pairs of consistent readings taken at different points of the pressed pellets.

Nuclear Magnetic Resonance Spectroscopy. ¹H NMR were recorded on a Bruker ACF 300 FT-NMR spectrophotometer operating at 300 MHz, while ¹³C NMR spectra, at 62.9 MHz. Deuterated solvents were used as indicated, and tetramethylsilane (TMS) was used as internal reference.

X-ray Photoelectron Spectroscopy. XPS analyses of polymer powders were performed by means of a VG ESCA/SIMLAB MKII with a Mg Kα radiation source (1253.6 eV). The binding energies were corrected for surface charging by referencing to the designated hydrocarbon C(1s) binding energy as 285.0 eV. Spectra deconvolutions were carried out using the Gaussian component with the same full widths at half-maximum (fwhm) for each component in a particular spectrum. Surface elemental stiochiometries were obtained from peak area ratios corrected with the appropriate experimentally determined sensitivity factors.

Scheme 1. Monomer Synthesis[a]
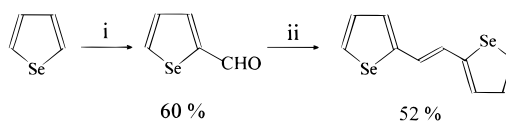
[a] Reagents and conditions: (i) PhMeNCHO/POCl₃/0 °C; (ii) TiCl₄Zn/THF/−30 °C.

Scanning Electron Micrographs. SEM of undoped polymers deposited on conducting ITO glass precoated with a thin layer of gold was run on a JEOL JSM-35CF scanning microscope.

Synthesis of 1,2-Bis(2-seleninyl)ethene (DSE). 1,2-Bis-(2-seleninyl)ethene was formed in two steps as depicted in Scheme 1. After recrystallization from hexane, yellow needles in 52% overall yield were obtained. Melting point: 152−153 °C. MS (EI, *m/e*, % intensity): 286 (M⁺, 100). UV−vis (hexane), λ_{max} (ε): 288 (9200), 340 (23 100), 356 (19 700). Anal. Calcd for C₁₀H₈Se₂: C, 41.98; H, 2.82; Se, 55.21. Found: C, 41.94; H, 3.01; Se, 55.27. ¹H NMR (300 MHz, CDCl₃): δ 6.98 (2H, s), 7.16−7.21 (4H, m), 7.82 (2H, dd, J_{2-3} 5.2 Hz, J_{3-4} 1.2 Hz).

Chemical Synthesis of Poly{1,2-bis(2-seleninyl)ethene}. Poly{1,2-bis(2-seleninyl)ethene} was synthesized by reacting 1 mol equiv of monomer with 4 mol equiv of anhydrous ferric chloride in a 0.5 M monomer solution in dry chloroform. Polymerization was carried out for 24 h under nitrogen at 0 °C. The as-synthesized polymer was deep blue, suggestive of it being in the doped state. The polymer powder was filtered under suction and washed successively with water and methanol under suction and then subjected to Soxhlet extraction with methanol and then acetone in turn for 24 h.

Dedoping and Doping of Polymer. Dedoping of the as-synthesized PDSE was effected by stirring the polymer powder vigorously in a solution containing hydrazine hydrate and deionized water (10 mL:10 mL) for 24 h. Thereafter, polymer powder was filtered under suction and subjected Soxhlet extraction using methanol and then acetone.

Chemical redoping of the dedoped polymer was carried out by stirring the dedoped polymer in 0.05 M ferric chloride in anhydrous nitromethane for 1 h under nitrogen.

Iodine doping of dedoped polymers was effected in an iodine chamber in the dark. Polymer pellets of known thickness and mass were placed inside the chamber for at least 24 h. The pellets were taken out periodically and weighed to determine iodine uptake, and their electrical conductivities were measured.

Electrochemical Polymerization. Polymer films were grafted on Pt foil or an indium tin oxide (ITO) glass electrode either by the potentiodynamic method, wherein the potential was cycled between −0.3 and +1.0 V at 50 mV s⁻¹, or by the galvanostatic method. It was observed that films obtained by the latter method were relatively thicker and more homogeneous. Electrochemical polymerization was performed under an argon atmosphere using an EG&G 273A potentiostat/galvanostat controlled by EG&G M270 electrochemical software. A three-electrode single compartment electrochemical cell consisted of a platinum foil (0.5 cm²) as the working electrode, a platinum wire as the counter electrode, and Ag/AgNO₃ (0.1 M in dry acetonitrile) as the reference electrode (0.34 V versus saturated calomel electrode (SCE). All experimental values in this report were corrected with respect to SCE. A current density of 0.5 mA cm⁻² was applied unless otherwise stated. Thin polymer films were grown galvanostatically under an argon atmosphere. Standard monomer solutions (0.02−0.1 M) in 0.1 M supporting electrolyte (Bu₄NClO₄ or Bu₄NBF₄) in acetonitrile were used for electropolymerization.

Results and Discussion

The chemical oxidative polymerization of 1,2-bis(2-seleninyl)ethene afforded 98% yield of a brownish-black polymer, which was found to be partially soluble in
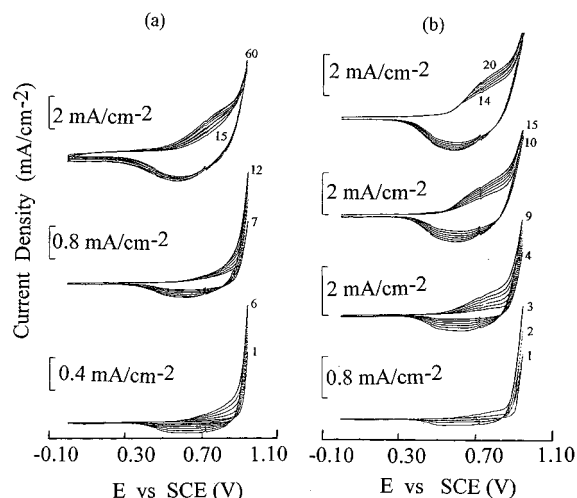
Figure 2. Cyclic voltammograms recorded during polymerization in different electrolytes: (a) 0.1 M n-Bu$_4$CF$_3$SO$_3$; (b) 0.1 M n-Bu$_4$BF$_4$.

Table 1. Bulk and Surface Stoichiometries of Dedoped and Doped PDSE

polymer	stoichiometries (bulk)	stoichiometries (surface)
P1	$C_{11.16}H_{8.40}Se_{2.00}Fe_{0.00}Cl_{0.17}I_{0.00}$	$C_{14.60}O_{0.51}Se_{2.00}Fe_{0.00}Cl_{0.00}I_{0.00}$
P2	$C_{11.14}H_{10.50}Se_{2.00}Fe_{0.32}Cl_{1.07}I_{0.00}$	$C_{19.64}O_{2.66}Se_{2.00}Fe_{0.08}Cl_{0.00}I_{0.00}$
P3	$C_{9.72}H_{6.28}Se_{2.00}Fe_{0.00}Cl_{0.00}I_{2.16}$	$C_{15.43}O_{1.56}Se_{2.00}Fe_{0.00}Cl_{0.00}I_{2.61}$

N-methyl-2-pyrrolidone, THF, DMF, and DMSO. Table 1 depicts a comparison of the bulk and surface stoichiometries of dedoped and doped PDSE. The determined bulk stoichiometries of dedoped PDSE (P1) fits closely to the expected values, while both the ferric chloride-doped (P2) and iodine-doped (P3) polymers show that a significant amount of dopant has been incorporated into the bulk polymer. Surface stoichiometries obtained from XPS revealed a higher than expected carbon and oxygen content for all three polymers P1, P2, and P3. The higher than expected carbon is ascribable to surface hydrocarbon contamination usually found in XPS studies,[20] while the higher oxygen content can be explained by bound water and or aerial oxidation during and after polymerization.[21] The selenium content in both bulk and surface determinations match the expected values well, suggesting minimal ring degradation of the selenophene moiety during the polymerization process.

Although electrochemical polymerization can be effected using either potentiostatic or galvanostatic methods, as well as cyclic voltammetry, in our studies, the last is the method of choice. Although this technique requires a longer reaction time to obtain of polymer films as compared with galvanostatic or potentiostatic methods, it was found advantageous since the electrochemical characteristics of the growing polymer can be monitored during the polymerization process. Polymerization in different mediums comprising different electrolytes, namely Bu$_4$NClO$_4$, Bu$_4$NBF$_4$, or Bu$_4$NSO$_3$CF$_3$, have been conducted. Figure 2a depicts a typical cyclic voltammograms of the electrochemical polymerization of 1,2-bis(2-seleninyl)ethene in Bu$_4$NSO$_3$CF$_3$ (0.1 M) at scan rate of 20 mV s^{-1}. Figure 2b shows the cyclic voltammograms of electrochemical polymerization using Bu$_4$NBF$_4$ (0.1 M) as electrolyte. The monomer oxidation potential of 1,2-bis(2-seleninyl)ethene is 0.93 V vs SCE, which is comparatively lower than selenophene (1.48 V)[22] and biselenophene (1.2 V)[23] under similar conditions, an indication of more extensive conjugation in our

monomer. Having determined the oxidation potential of the monomer, polymerization is then initiated by setting the potentiostat to cycle from 0.00 to 0.95 V versus saturated calomel electrode (SCE) repeatedly.

No apparent redox peaks were observed during the first scan. As the number of scans increases, the cathodic peak increases in intensity. An anodic peak at approximately 0.75 V, corresponding to the oxidation of PDSE is observed. As polymerization proceeds, the peak current increases in the successive scans, indicating the growth of polymer on the surface of the electrode. The increase in anodic peak current is enhanced in the presence of Bu$_4$NBF$_4$ (Figure 2b) electrolyte compared to Bu$_4$NSO$_3$CF$_3$. It is observed that in Bu$_4$NSO$_3$CF$_3$ (Figure 2a) electrolyte, the polymerization rate is slightly slower. A similar observation has been reported for the analogous thiophene polymer,[24,25] though no satisfactory rationalization was detailed.

Electrochemistry of Poly{1,2-bis(2-seleninyl)-ethene}. The electrochemistry of the PDSE obtained above is studied in monomer-free solution. During the doping process, the polymer film deposited onto platinum foil is cycled repeatedly between the conducting (oxidized) and nonconducting (neutral) state without showing significant decomposition of the material. Strong electrochromism is observed when the polymer is cycled from a potential of -0.3 to $+0.8$ V versus SCE. A deep blue adhesive polymer film is obtained on an ITO glass plate/platinum electrode when in its doped form. Upon reduction to its neutral dedoped form, the polymer film took on a violet coloration.

Both p- and n-doping studies of PDSE have been carried out in acetonitrile using tetra-n-butylammonium perchlorate, tetra-n-butylammonium fluoroborate, tetra-n-butylammonium triflate, and lithium perchlorate as electrolyte (0.1 M).[26] A continuous potentiostatic scan sweeping from 0 to 0.9 V (p-doped region) and then to -1.8 V (n-doped region) was applied. The cyclic voltammogram of PDSE showing both p- and n-doping at different scan rates is displayed in Figure 3. During the p-doping process, the polymer oxidation potential (E_{pa}) and reduction potential (E_{pc}) are 0.75 and 0.67 V, respectively, at a scan rate of 50 mV/s for all electrolytes. The influence of electrolyte on the p-doping activity is negligible since the doping mechanism is highly reversible. It is commonly observed from the spectrum that both E_{pa} and E_{pc} increase slightly as the scan rate is increased. Similarly, for the n-doping process, both E_{pa} and E_{pc} shift to more negative potentials when the scan rate is increased. The electrolyte shows a significant influence in the n-doping process, whereby larger shifts in E_{pa} and E_{pc} are observed in ClO$_4^-$ (Figure 3b) and CF$_3$SO$_3$- (Figure 3c). By subtracting E_{pc} from E_{pa}, the result is a difference in peak potential of approximately 80 mV at a scan rate of 50 mV s^{-1}. This phenomenon is commonly observed in the electrochemistry of conducting polymers, which may be attributed to a number of factors, including the ease of diffusion of dopant ion in and out of the polymer film, film thickness, and reorganization of polymer chains in the transition between the rigid planar oxidized state and the flexible neutral states.[27]

From coulometric measurements shown in Table 2, the p-doping process is found to be reversible. The n-doping process on the other hand is less reversible due to its large Coulombic imbalance for the oxidation and reduction process. The peak current density is
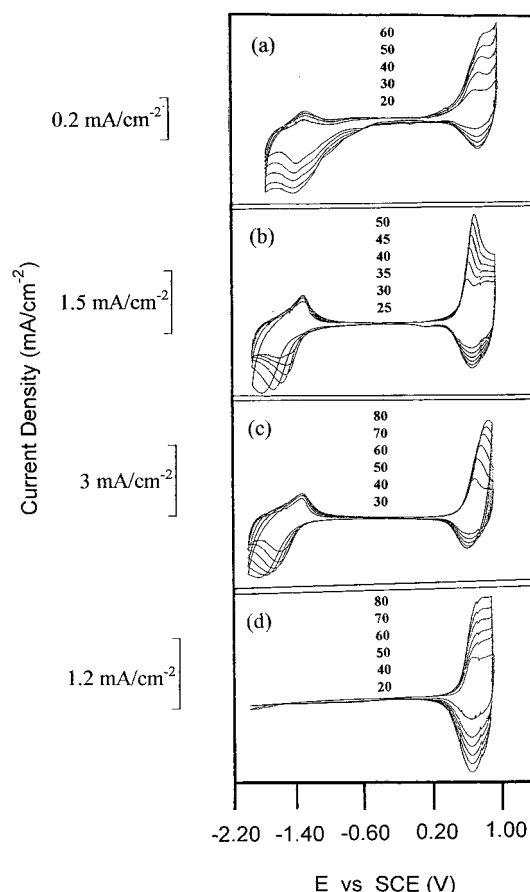
Figure 3. Cyclic voltammograms of PDSE film electrodeposited onto platinum foil in monomer-free solution using different electrolytes (0.1 M): (a) n-Bu$_4$BF$_4$; (b) n-Bu$_4$ClO$_4$; (c) CF$_3$SO$_3$-n-Bu$_4$$^+$; (d) LiClO$_4$.

Table 2. Integrated Charge of the Anodic Current for p-Doping (0−0.95 V) and Cathodic Current for n-Doping (−1.0 to −2.0 V) Processes, from the Cyclic Voltammograms at Various Scan Rates (20, 30, 40, 50, and 60 MV s^{-1})

| scan rate (mV/s) | CV charge of PDSE (mC) | | | | | |
| | p-doping | | | n-doping | | |
	oxidation	reduction	total	oxidation	reduction	total
20	3.815	−1.324	5.139	−8.246	9.814	18.06
30	3.451	−1.394	4.845	−6.754	0.744	7.498
40	3.397	−1.279	4.676	−6.023	0.586	6.609
50	3.085	−1.178	4.263	−5.580	0.607	6.187
60	2.960	−1.025	3.985	−4.955	0.609	5.564

Table 3. Changes in Peak Currents and Redox Potentials of PDSE during p- and n-Doping at Different Scan Rates (20, 30, 40, 50, and 60 MV s^{-1})

| scan rate (mV/s) | p-doping of PDSE | | | | n-doping of PDSE | | | |
	I_{pa} (mA)	I_{pc} (mA)	E_{pa} (V)	E_{pc} (V)	I_{pa} (mA)	I_{pc} (mA)	E_{pa} (V)	E_{pc} (V)
20	0.138	0.114	0.695	0.654	0.717	0.0286	−1.503	−1.405
30	0.228	0.238	0.689	0.664	0.214	0.124	−1.531	−1.388
40	0.305	0.333	0.732	0.672	0.238	0.181	−1.546	−1.384
50	0.362	0.381	0.753	0.670	0.276	0.247	−1.549	−1.377
60	0.429	0.476	0.776	0.676	0.305	0.286	−1.554	−1.373

observed to scale linearly with increasing scan rate (Table 3). A linear plot of current density versus scan rate is obtained for both the p- and n-doped processes, which is characteristic of electroactive polymers where the current is not diffusion controlled.[28]

During p-doping, charges are removed from the valence band of PDSE when the applied potential reaches 0.43 ± 0.01 V. This is characterized as the onset potential for the oxidation of PDSE and can be correlated to the highest occupied states in the valence band (HOMO). The charge that is removed is balanced by ionic species that transfer from the electrolyte to the polymer, thus ensuring overall electrical neutrality. From the anodic and cathodic peak potentials, we determine the average potential necessary for the formation of the doped state of PDSE to be 0.71 V. The onset potential for n-doping is observed at −1.20 ± 0.01 V. This onset voltage correlates with the lowest unoccupied states (LUMO) in the conduction band. Thus, the difference between the HOMO and LUMO leads to the evaluation of the band gap of PDSE to be 1.63 ± 0.01 eV.[29] This value is in good agreement with the band gap derived from optical data described below.

Optical Studies of PDSE. The UV−vis absorption spectrum of dedoped PDSE film on ITO glass exhibits an absorption maximum (λ_{max}) at 526 nm. This broad absorption band lies between 360 and 740 nm, which corresponds to the $\pi \rightarrow \pi^*$ interband transition. Most conjugated polymers are generally characterized by a broad absorption band due to their intrinsic energetic disorder. This disorder is produced primarily by the variation of conjugation length in polymer segments. The band gap of PDSE derived from this interband transition is deduced from the energy absorption edge of the spectrum using the expressions[30]

$$\alpha h\nu = A(h\nu - E_g)^{1/2}$$

$$(\alpha h\nu)^2 = A^2(h\nu - E_g)$$

$$(\alpha h\nu)^2 = (\text{const})(h\nu - E_g)$$

In the expression, α is the absorption coefficient near the absorption edge, A is a proportionality constant, and E_g is the band gap of the polymer. By plotting $(\alpha h\nu)^2$ versus $h\nu$ for the PDSE film in the region between 668 and 746 nm (band edge region), followed by extrapolation of the plot to zero, a direct band gap of 1.6 eV is obtained. Upon comparisons of neutral dedoped polyselenophene films with PDSE, polyselenophene exhibits a λ_{max} value of 440 nm and a band gap of 2.0 eV.[22] PDSE on the other hand is significantly red shifted and its derived optical band gap is the lowest among the selenophene-containing polymers reported so far. The coplanarity of the selenophene rings is expected to be slightly enhanced in PDSE as compared to polyselenophene because the separation between neighboring selenophene rings is larger. Thus it is believed that the ethenyl spacer plays an important role by elevating the top of the valence band to a relatively higher energy level, thereby reducing the band gap energy.

Parts a and b of Figure 4 depict the optical absorption spectral changes of PDSE taken in situ during electrochemical p-doping and n-doping as a function of applied potential. As evident from Figure 4a, when PDSE is p-doped electrochemically, the peak height of the interband transition decreased and appears shifted to higher energy as doping levels are increased. In the neutral states, only a single absorption peak is observed at about 2.36 eV due to interband excitation and the polymer is purplish red in color, while the doped form is blue in color when cycled to +1.10 V vs Ag|AgCl
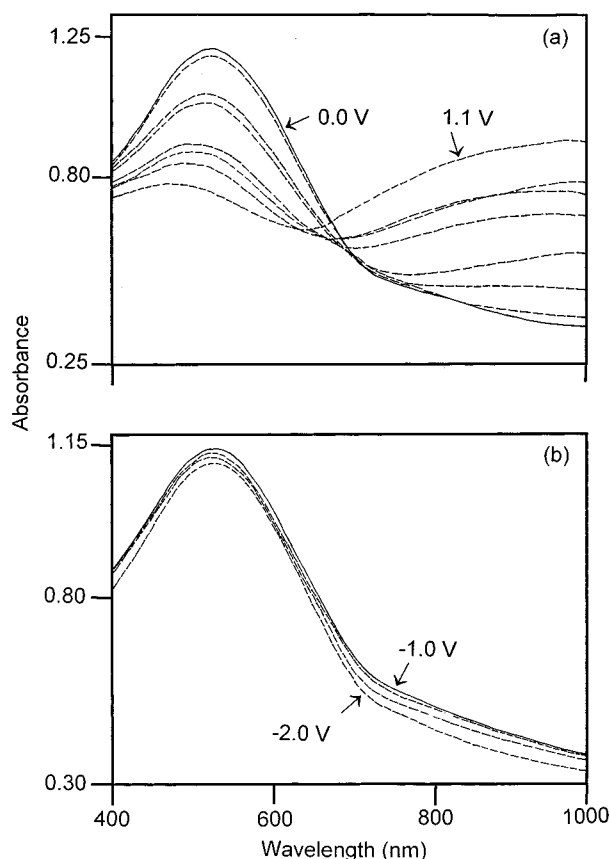
Figure 4. In situ UV−vis absorption of PDSE recorded at different potentials during (a) p-doping and (b) n-doping.

electrode. These remarkable changes of the absorption spectrum upon doping are typical characteristics of conducting polymers. Although we are unable to observe any p-type polaron bands within the UV−vis range, at least one absorption peak is likely to be present at an energy around 1.2 eV by scanning to the near-infrared region.

n-Doping of PDSE is carried out in situ by cycling the potential to −1.80 V vs Ag|AgCl electrode. When the polymer is cycled to the negative potential, the absorption peak at 526 nm remained unchanged and shows no tailing of bands toward higher wavenumbers. This could be attributed to the instability of the n-doped state.

Surface Morphology of Electrochemically Doped PDSE. Scanning electron micrographs of PDSE films grafted on an ITO glass plate appear differently depending on sample thickness, although a distinctly globular morphology is evident. A thin polymer film (less than 5 μm) is grafted galvanostatically from monomer solution (0.01 M) in 0.1 M electrolyte (ClO$_4$⁻) using a current of 0.1 mA for 40 s. To generate thicker films (> 1 μm), the time for deposition was increased to 120 s, keeping all other conditions constant. Figure 5a shows that when PDSE is grafted as thin films, SEM micrographs reveal that the surface is very homogeneous. The surface consists of small spherical granules that are neatly packed close to one another. The size of each individual granule ranges from 0.05 μm to 0.3 μm. A thick polymer film, on the other hand, shows more irregular structure, as seen from Figure 5b. Numerous globules are randomly dispersed on the surface. When magnified 30 000 times, the surface shows that each globule consists of numerous individual
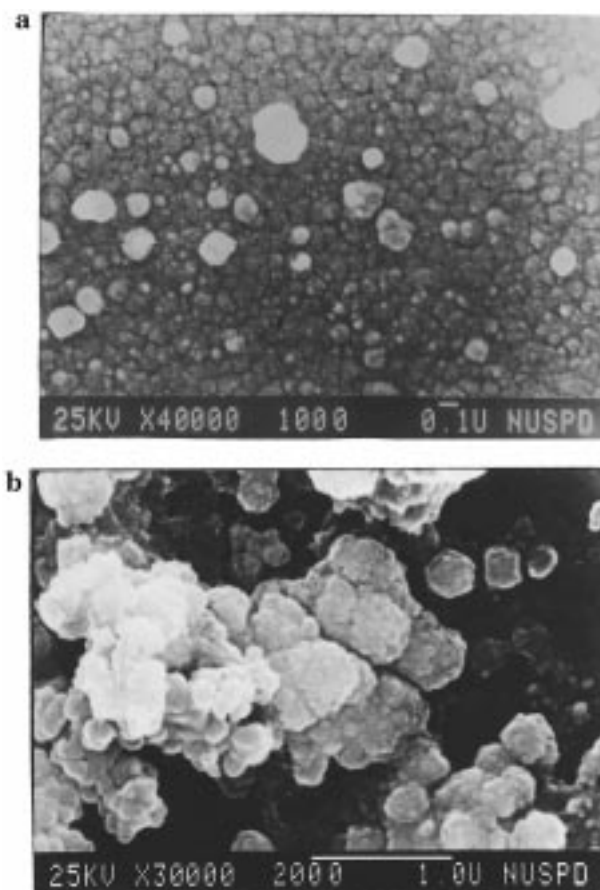

Figure 5. SEM micrographs of PDSE deposited electrochemically on ITO glass of different thicknesses: (a) thin transparent film; (b) thick film.

granules that are stacked on top of one another. This nonuniformity of the polymer surface may be due to poor distribution of charge on the ITO glass, which causes the polymer growth rate to be nonuniform.

FTIR of Monomer and Polymers. The FTIR spectrum of DSE and its respective polymers are shown in Figure 6. The monomer shows a band at 679 cm⁻¹, which corresponds to the α-CH out of plane bend of the aromatic ring. In the dedoped polymer, the α-CH out of plane bend is significantly reduced compared to the β-CH out of plane bend at 786 cm⁻¹, implying that the polymerization of DSE has occurred predominantly through α−α' couplings. For electrochemically (BF4⁻) doped polymer, C−H ring stretching at 3054 cm⁻¹ as well as −C=C− and aromatic ring stretching at 1643 and 1531 cm⁻¹ are observed. Intense bands at 1360, 1314, 1090, and 1014 cm⁻¹ are attributed to the vibrational mode in the BF$_4$⁻-doped selenophene ring. For chemically doped polymers, the spectrum shows significantly broad bands at 1017, 1103, 1189, 1293, 1345, and 1379 cm⁻¹ and 1036, 1109, 1181, 1254, 1327, and 1381 cm⁻¹, which are known to be the doping-induced bands of ferric chloride and iodine-doped polymer, respectively. The FTIR spectra of the doped polymers are not only broadened but also shifted toward lower frequencies with respect to their dedoped polymer. This shift in the infrared bands to lower energies indicates bond weakening, arising from the removal of electron density from the π-bonding orbitals of the selenophene ring as a result of the oxidation of the polymer. This is corroborated later in X-ray photoelectron spectroscopic analysis (XPS), which gives evidence
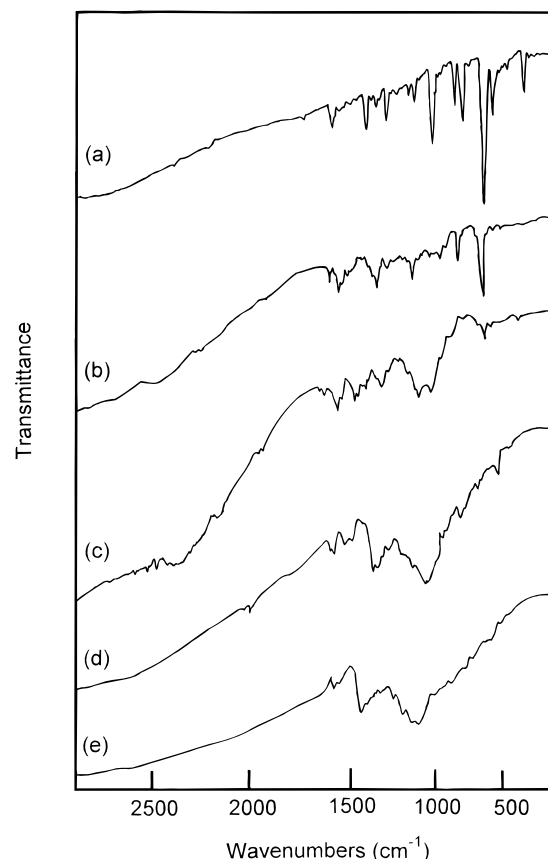
Figure 6. Fourier transform infrared spectrum of (a) monomer DSE, (b) dedoped PDSE, (c) $FeCl_3$-doped PDSE, (d) I_2-doped PDSE, and (e) electrochemically doped PDSE in 0.1 M Bu_4NBF_4.

Figure 7. TGA and DTG of (a) P1 (dedoped PDSE), (b) P2 ($FeCl_3$-doped PDSE), and (c) P3 (iodine-doped PDSE).

for the formation of a delocalized positive charge on the selenium in doped PDSE.

Macroscopic dc Conductivity of Doped Polymers. DC conductivity measurements are carried out on compressed powders of chemically doped PDSE using a four-point probe. Dedoped PDSE, P1, is nonconducting ($<10^{-5}$ S cm^{-1}). Iodine-doped PDSE, P3, shows a higher conductivity of 0.27 S cm^{-1} than ferric chloride-doped PDSE, P2 (0.11 S cm^{-1}). This conductivity value is slightly higher than that of its thiophene analogue, poly{1,2-bis(2-thienyl)ethene} (0.1),[31] though much higher than polyselenophene (10^{-2} S cm^{-1}).[22]

Thermogravimetric Analysis of Polymers. TGA spectra of the dedoped polymer (P1) is shown in Figure 7. Degradation occurs through a single weight loss step in both air and nitrogen. In air, thermal oxidative degradation occurs over a range of temperature from 240 to 570 °C. The maximum rate of degradation is observed at 470 °C. The amount of weight loss is 91.4% when the temperature reaches 570 °C. Under a nitrogen atmosphere, the rate of degradation is comparatively lower and degrades over a temperature range of 250–600 °C, accounting for a weight loss of 98.6%. The maximum rate of degradation remained unchanged in nitrogen.

TGA spectra of ferric chloride-doped PDSE (P2) shows that it is thermally less stable than the dedoped polymer (P1). It degrades gradually through a single weight loss step, and its maximum rate of degradation occurs at 371 °C, which is nearly 100 °C lower than P1. Moreover P2 leaves behind a significantly large amount of resi-
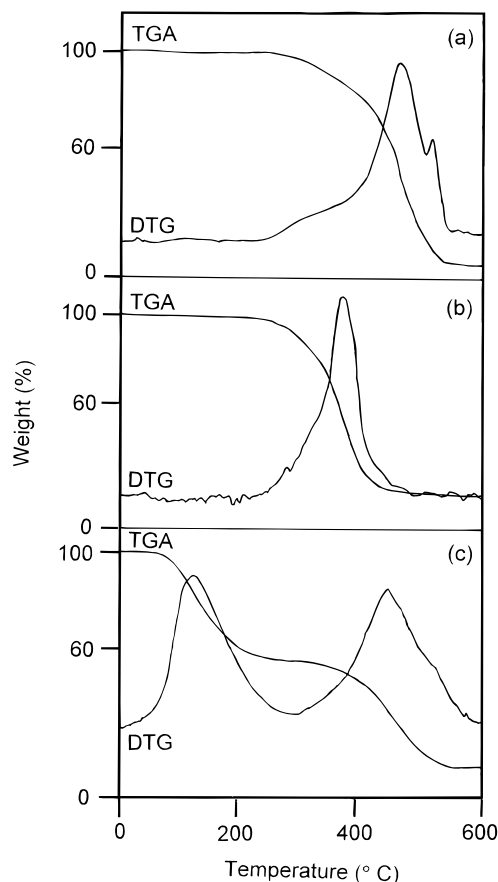
due: 36.5% at 500 °C in nitrogen and 19.6% at 600 °C.

Iodine-doped PDSE (P3) degrades over two weight loss steps both in air and in nitrogen. The first weight loss step from ambient temperature to 260 °C is primarily due to the explusion of iodine dopants from the polymer backbone. The second weight loss step at 260–600 °C is due to thermal degradation of the bulk polymer. The temperature at maximum rate of degradation is 400 °C. Comparisons made between the doped and undoped polymers shows that the temperature at maximum rate of degradation for P1 is highest, followed by P3 and P2. Therefore, the rate of thermal oxidative degradation is greater in the doped polymers.

X-ray Photoelectron Spectroscopy of Polymers. The C(1s) envelopes of P1, P2, and P3 were seen to display similar shapes with a tailing toward the higher binding energy, which is indicative of the long-range disordered conjugation present. The C(1s) spectrum has been deconvoluted into three main environments: C–C or C–H (285.0 eV), C–O (286.3 eV), and C=O (287.9 eV) with full wave half-maximum (fwhm) of 1.60 eV and their respective area ratios being 74.9, 17.7, and 7.3%. It was observed that the main environment attributed to C–C/C–H is of higher percentage than the surface-oxidized portion of the polymer at higher binding energy, which corresponds to only ca. 25%. The presence of these two minor environments can be due to aerial oxidation during polymerization.[32]

The O(1s) envelope has been deconvoluted into three main environments. The first component is assigned to C=O at 532.2 eV with a fwhm of 1.8 eV. The second and third environment at 533.3 and 535.1 eV are assigned as C–O and H_2O, respectively.[33] However, the

Table 4. XPS Binding Energies (BE) and Full Wave Half-Maximums (fwhm) of Environments and Their Respective Areas for C(1s), Se(3d), and O(1s) Core Levels

binding energies (eV)	fwhm (eV)	assignment	areas		
			P1	P2	P3
C(1s)					
285.00 ± 0.00	1.60	C–C, C–H, or C=C	73.90	68.58	69.95
286.30 ± 0.02	1.60	C–O	18.15	21.56	18.78
287.95 ± 0.00	1.60	C=O	7.95	9.86	11.27
Se(3d)					
57.93 ± 0.00	1.10 ± 0.10	$Se_{5/2}$–C	40.84	41.66	45.49
58.56 ± 0.00	0.90 ± 0.10	$Se_{3/2}$–C	27.61	25.41	30.04
59.16 ± 0.00	0.90 ± 0.10	$Se_{5/2}^{+}$–C	19.26	19.23	14.65
59.79 ± 0.00	1.00 ± 0.02	$Se_{3/2}^{+}$–C	12.28	13.70	9.81
O(1s)					
532.15 ± 0.06	1.80	O=C	35.71	48.96	31.05
533.35 ± 0.05	1.80	O–C	55.01	38.48	53.18
535.10 ± 0.00	1.80	O–H_2O	9.28	12.56	15.77
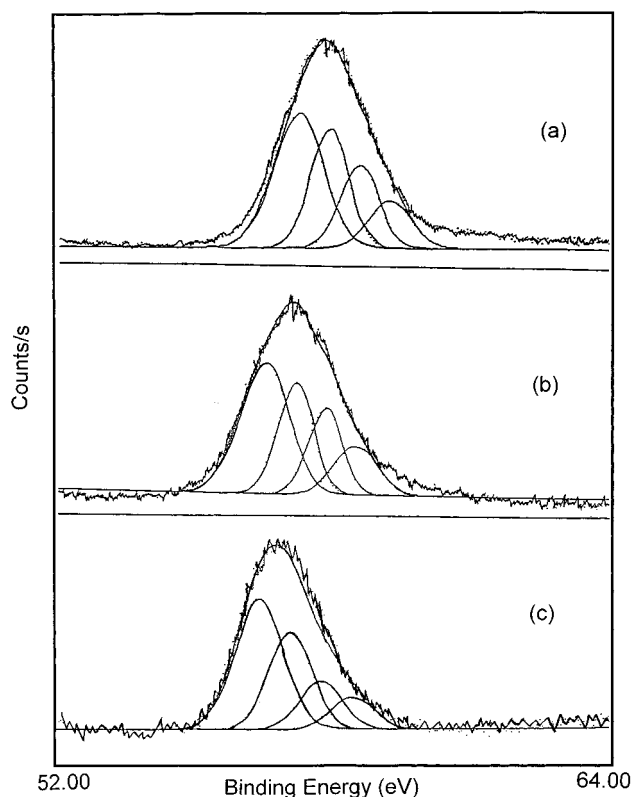
Figure 8. Deconvoluted XPS spectra of the Se(3d) region of (a) P1 (dedoped PDSE), (b) P2 (FeCl₃-doped PDSE), and (c) P3 (iodine-doped PDSE).

amount of aerial oxidation is low, as seen from surface stoichiometries in Table 4.

The core level spectrum of the Se(3d) envelope has been studied in some detail in this work, as little research work was performed so far. Arising from spin−orbit coupling effects, the Se(3d) envelope (Figure 8) of dedoped polyselenophene consists of a doublet that corresponds to Se(3d$_{5/2}$) and Se(3d$_{3/2}$), with the latter at a higher binding energy with their splitting evaluated to be at 0.6 ± 0.1 eV.[34] Since their respective area ratio is 3:2, the shape of the Se(3d) peak is asymmetrical with tailing toward the higher binding energy. The fwhm of each environment gives a best fit at 1.00 ± 0.2 eV.

The Se(3d) spectrum has been deconvoluted into four main environments: C−Se(3d$_{5/2}$), C−Se(3d$_{3/2}$), C−Se^{+}-(3d$_{5/2}$), and C−Se^{+}(3d$_{3/2}$), at binding energies of 57.9, 58.5, 59.2, and 59.7 eV, respectively.[35] The chemical shift between C−Se and C−Se^{+} is 1.2 ± 0.1 eV. The
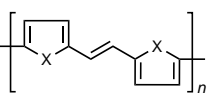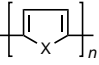
evidence for a single positive charge on the selenium metal was compared with its thiophene analogues[36] and was found to be satisfactory. The extent of doping in the doped polymers P2 and P3 can be evaluated from the relative area ratio of C−Se^{+} over C−Se. The highest ratio of 0.65 has been obtained by P3, which corresponds to the iodine-doped polymer (0.27 S cm^{-1}), followed by P2, which is ferric chloride-doped (0.11 S cm^{-1}) with a marginally lower ratio of 0.64. The dedoped polymer, P1, which is nonconducting, gives a ratio of 0.21.

The I(3d$_{5/2}$) envelope has been deconvoluted into three components having a fwhm of 1.6 eV. The component at 619.4 eV is assigned to be the I$_3^{-}$ species, while the next environment at 620.8 eV is due to the presence of I$_5^{-}$.[37] The last component has the smallest area ratio at a binding energy of 621.8 eV, which is attributed to the covalently bonded iodine or molecular iodine. Since I$_3^{-}$ is more chemically stable than I$_5^{-}$ species, the percentage area ratio for the latter is generally lower.

It is our aim to obtain a clear picture of how significantly the heteroatom influences the mean effective conjution in the polyheterocycle. We want to compare the physical, optical, and electronic properties of polyfuran, polythiophene, and polyselenophene. Researchers have reported the band gap of polyheterocycles to be in the following order: polyfuran (2.4 eV) > polythiophene (2.1 eV) > polyselenophene (2.0 eV). The UV−vis analysis of these homopolymers shows a general trend toward longer wavelength in the order polyfuran < polythiophene < polyselenophene. These physical properties suggest that polyselenophene is a very promising candidate for application as a conductive material.

As we modify the homopolymer by introducing an ethylene spacer between two heterocycles, we obtain a resulting polymer having an even lower band gap energy. The purpose of inclusion of the flexible spacer is to help minimize steric effects between the arylene rings. As seen from Table 5, upon inclusion of the ethylene spacer, PSDE, polymer **V** and polymer **VI** show a diminished band gap energy and their UV−vis absorption have been significantly red shifted, suggesting an increase in extent of conjugation in the polymer chain. Therefore, the extent of torsional strain between the neighboring arylene rings is expected to be reduced. Now if we compare the heteroatoms (O, S, and Se) in the polyheterocycle, we noted that different heteroatoms contribute different properties in the polymer. The Se atom is found to be most favorable, giving the lowest band gap energy, and has a greater extent of conjugation, as reflected from UV−vis absorption.

Table 5. Comparisons between the UV−Vis, Band Gaps, and Electrical Conductivities of Various Polymers

polymer structure	hetero-atom X	λ_{max} (nm)	band gap (eV)	conductivity (S cm^{-1})
	Se	526	1.6	0.27
	S	515	1.9	0.13
	O			2×10^{-4}
	Se	440	2.0	3.7×10^{-2}
	S	480	2.1	1000
	O		2.35	2×10^{-3}

Conclusion

Poly{*trans*-1,2-bis(2-seleninyl)ethene} (PDSE) was successfully generated both chemically and electrochemically. Chemical polymerization using ferric chloride afforded polymer in high yield. Upon doping with iodine, PDSE attained a maximum conductivity of 0.27 S cm^{-1}. The conductivity plot had shown that conductivity varied with the amount of dopant absorbed onto the polymer. Electrochemically synthesized PDSE using ClO$_4^-$ or BF$_4^-$ counteranion leads to a deep blue polymer film when doped and purple when undoped. Optical studies of dedoped PDSE on ITO glass show a bathochromic shift of its λ_{max} value with respect to polyselenophene from 440 to 560 nm. Its optically derived band gap (1.6 eV) was also lower than polyselenophene (2.0 eV). These clearly prove that the presence of the ethenyl spacer in the macromolecular backbone contributed to a lowering of the band gap energy. SEM micrographs revealed the polymer surface to be homogeneous and densely packed in thin the film. A thicker film showed a more irregular structure. TGA results showed that the rate of thermal oxidative degradation was greater in the doped polymers than in the undoped form. XPS studies of PDSE had been studied in detail. In particular, the Se(3d) spectra can be deconvoluted into four main environments: C−Se(3d$_{5/2}$), C−Se(3d$_{3/2}$), C−Se$^+$(3d$_{5/2}$), and C−Se$^+$(3d$_{3/2}$) with respective binding energies at 57.9, 58.5, 59.1, and 59.7 eV. Further work involving the incorporation of conjugative spacers such as the ethynyl moiety is now in progress in our laboratory and will be reported in due course.

References and Notes

(1) Glenis, S.; Benz, M.; Legoff, E.; Schindler, J. L.; Kannewurf, C. R.; Kanatzidis, M. G. *J. Am. Chem. Soc.* **1993**, *115*, 12519.
(2) Ferraris, J. P.; Bravo, A.; Kim, W.; Hrncis, D. C. *J. Chem. Soc., Chem. Commun.* **1994**, 991.
(3) Hillman, A. R.; Mallen, E. F. *J. Electroanal. Chem.* **1990**, *281*, 109.
(4) Tourillon, G.; Dartyge, E.; Guay, D.; Mahatsekake, C.; Andrieu, C. G.; Bernstorff, S.; Braun, W. *J. Electrochem. Soc.* **1990**, *137*, 1827.
(5) (a) Ng, S. C.; Chan, H. S. O.; Sarkar, A.; Leong, L. S. *J. Mater. Sci. Lett.* **1996**, *4*, 664. (b) Ng, S. C.; Chan, H. S. O.; Sarkar, A.; Mazaki, Y.; Kobayashi, K. *J. Mater. Sci. Lett.* **1996**, *15*, 1684.
(6) (a) Dian, G.; Barbey, G.; Decroix, B. *Synth. Met.* **1986**, *13*, 281. (b) Mahatsekake, C.; Catel, J. M.; Andrieu, C. G.; Ebel, M.; Mollier, Y. *Phosphorus, Sulfur Silicon* **1990**, *47*, 35.
(7) Morel, J.; Paulmier, C.; Garreau, M.; Martin, G. *Bull. Soc. Chim. Fr.* **1971**, 4497.
(8) Iwatsuki, S.; Kamei, N.; Kubo, M. *Chem. Soc. Jpn., Chem. Lett.* **1992**, 1551.
(9) (a) Kossmehl, G. *Makromol. Chem., Macromol. Symp.* **1986**, *4*, 45. (b) Peter, L.; Evers, W.; Van Der Borght, M.; Jacobs, S.; Geise, H. J. *Polymer* **1993**, *21*, 4589. (c) Bolognesi, A.; Catellani, M.; Porzio, W.; Galanini, R.; Musco, A.; Pontellini, R. *Polymer* **1993**, *19*, 4150.
(10) Kossmehl, G.; Thomas, G. *Macromol. Chem. Phys.* **1994**, *195*, 3655.
(11) Eckhardt, H.; Shacklette, L. W.; Jen, K. Y.; Elsenbaumer, R. L. *J. Chem. Phys.* **1989**, *91*, 1303.
(12) Catellani, M.; Luzzati, S.; Sperani, F. *Synth. Met.* **1993**, *55*, 1189.
(13) Kossmehl, G.; Thomas, G. *Makromol. Chem.* **1992**, *193*, 335.
(14) Onoda, M.; Iwasa, T.; Kawai, T.; Yoshino, K. *J. Phys. D: Appl. Phys.* **1991**, *24*, 2076.
(15) Tsumura, A.; Koezuka H.; Ando, T. *Appl. Phys. Lett.* **1986**, *49*, 1250.
(16) Lobek, W.; Kiess, H.; Egli, M. *Synth. Met.* **1988**, *22*, 265.
(17) Tsumura, A.; Koezuka, H.; Ando, T. *Synth. Met.* **1988**, *25*, 11.
(18) Gerff, K.; Simon, J. H. *J. Mater. Chem.* **1995**, *5* (3), 447.
(19) Benzoari, M. D.; Kovacic, P.; Gronowitz, S.; Hoernfeldt, A. B. *J. Polym. Sci., Polym. Lett. Ed.* **1981**, *19* (7), 347.
(20) Chan, H. S. O.; Ng, S. C.; Sim, W. S.; Tan, K. L.; Tan, B. T. G. *Macromolecules* **1992**, *25*, 6029.
(21) Chan, H. S. O.; Toh, C. S.; Gan, L. M. *J. Mater. Chem.* **1995**, *5* (4), 631.
(22) Spyridon, G.; David, S. G.; Arthur, J. F. *J. Appl. Phys.* **1987**, *62* (1), 190.
(23) Shabana, G.; Galal, A.; Mark, H. B.; Hans Zimmer, J. R.; Gronowitz, S.; Hornfeldt, A. B. *Phosphorus, Sulfur Silicon.* **1989**, *42,* 171.
(24) Robert, A. H.; Marcus, J. S. *Electrochim. Acta* **1988**, *33* (10), 1303.
(25) John, B.; Ivaska, A. *Synth. Met.* **1991**, *44*, 9.
(26) Mitsuyoshi, O.; Hiroshi, N.; Shigenori, M.; Katsumi, Y. *J. Appl. Phys.* **1993**, *73* (6), 2859.
(27) Meerholz, K.; Heinze, J. *Angew. Chem., Int. Ed. Engl.* **1990**, *29*, 692.
(28) Genies, E.; Bidan, G.; Diaz, A. F. *J. Electroanal. Chem.* **1983**, *149,* 113.
(29) Wen, C. C.; Samson, A. J. *Macromolecules* **1995**, *28*, 465.
(30) Johnson, E. G. In *Semiconductors and Semimetals*; Willardson, R., Beer, A. C., Eds.; Academic: New York, 1967; Vol. 3, p 153.
(31) Marinella, C.; Silvia, L.; Alfredo, M.; Fabio, S. *Synth. Met.* **1994**, *62,* 223.
(32) Chan, H. S. O.; Gan, L. M.; Chew, C. H.; Ma, L. R.; Seow, S. H. *J. Mater. Chem.* **1993**, *3* (11), 1109.
(33) Chan, H. S. O.; Ng, S. C.; Leong, L. S.; Tan, K. L. *Synth. Met.* **1995**, *137*, 1827.
(34) Rupp, H.; Werser, U. *Bioinorg. Chem.* **1975**, *5* (1), 21.
(35) Nefedow, V. I.; Sergushin, N. P.; Salyn, Y. V.; Band, I. M.; Trzaskovskaya, M. B. *J. Electron. Spectrosc. Relat. Phenom.* **1975**, *7* (2), 175.
(36) Tourillon,G.; Dartyge, E.; Guay, D. *J. Electrochem. Soc.* **1990**, *137*, 1827; *Phosphorus, Sulfur Silicon.* **1989**, *42,* 171.
(37) Salaneck, W. R.; Thomas, H. R.; Bigelow, R. W.; Duke, C. B.; Plummer, E. W.; Heeger, A. J.; MacDiarmid, A. G. *J. Chem. Phys.* **1980**, *72* (6), 3674.